

ASSOCIATION OF GROUND EFFECT AND LEV INSTABILITY AROUND PARALLEL OSCILLATING FOILS

Ahmet Gungor^{1†}, Suyash Verma^{2†}, Muhammad Saif Ullah Khalid^{3§}, Arman Hemmati^{4†}

[†]Department of Mechanical Engineering, University of Alberta, Edmonton, AB, Canada T6G 2R3

[§]Department of Mechanical and Mechatronics Engineering, Lakehead University, Thunder Bay, ON P7B 5E1, Canada

¹gungor@ualberta.ca, ²suyash@ualberta.ca, ³mkhalid7@lakeheadu.ca, ⁴arman.hemmati@ualberta.ca

ABSTRACT

Instabilities of leading edge vortices (LEVs) on two side-by-side pitching foils are numerically examined at Reynolds number of 8000. This study demonstrates that ground effect plays a pivotal role in altering LEV dynamics, ultimately influencing the three-dimensional instability characteristics around the foils. Under moderate ground effect, LEVs remain attached to the foil, developing spanwise undulations due to surface interactions, before reaching the trailing edge. Conversely, extreme ground effect coincides with detachment of LEVs from the surface, which significantly reduces their interactions, preserving their two-dimensional structure until their merger with the trailing edge vortex. This hints at the complex dynamics of ground effect, in which the system experience suppression and excitement of instabilities depending on the body-body proximity.

INTRODUCTION

Understanding the fundamental aspects of vortex dynamics and wake interactions is crucial for unraveling the complex flow phenomena that frequently occur in both natural environments and industrial applications (Lewke *et al.*, 2016). The mechanisms governing the formation and evolution of vortex filaments, along with their interactions with the surrounding environment, are garnering increased attention due to their pivotal role in aircraft wake dynamics (Lewke & Williamson, 1998; Cerretelli & Williamson, 2003; Meunier *et al.*, 2005). Research by Lewke & Williamson (1998) on counter-rotating vortex pairs showed that short-wavelength instabilities developed cooperatively within these structures. It further explored the long-term flow evolution, highlighting interactions between short-wavelength and long-wavelength instabilities. In a separate investigation, Cerretelli & Williamson (2003) detailed the physical mechanisms that govern the merging process of two co-rotating vortices, which sequentially experienced phases of diffusion, convection, and merging. This study revealed that induced velocities from the asymmetric vorticity field of the vortex pair drove the centroids of the vortices towards each other, ultimately facilitating their merger.

The study of instabilities in wake structures has recently gained attention due to its relevance in understanding propulsion characteristics in insect flight and aquatic locomotion (Deng *et al.*, 2016). Deng & Caulfield (2015) observed that the transition from symmetric reverse von Kármán wakes to deflected wake modes coincided with the emergence of three-dimensional instability features and increased thrust production. Verma & Hemmati (2021) provided both quantitative

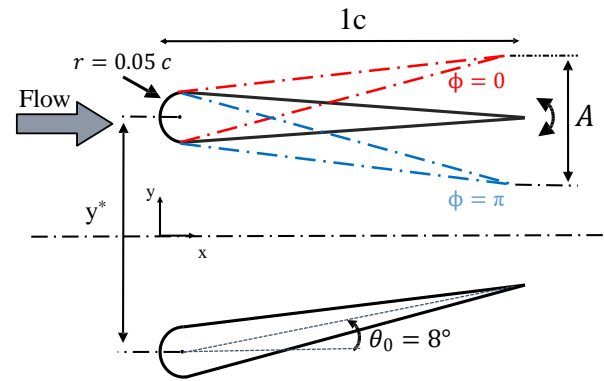


Figure 1. Demonstration of the in-phase and out-of-phase pitching motions of parallel oscillating foils (not to scale).

and qualitative evidence linking the spanwise undulation of the leading edge vortex to the elliptic instability of vortex pairs in the wake of foils performing simultaneous heaving and pitching motions. Their findings shed light on the relationship between spanwise instability and the development of streamwise vortical structures, enhancing our understanding of fluid dynamics in biologically inspired propulsion. A more recent study by Verma *et al.* (2023) explored a broader range of parametric spaces to examine the relationship between foil kinematics and three-dimensional characteristics of its wake. This study identified two distinct mechanisms that govern the growth of secondary structures, and delineated two major pathways characterizing the transition between these mechanisms. Thus, it provides deeper insights into the complex dynamics of wake instability.

Despite considerable efforts to characterize instabilities around a single oscillating foil, the impact of ground effect on flow instabilities of oscillating foils remain relatively unexplored. Here, we define ground effect as the impact of one foil on the flow dynamics around another. Quinn *et al.* (2014) showed that the flow around a pitching foil is significantly affected by the presence of a solid wall, particularly when placed very close to the foil. However, they did not explore the dynamics of the LEVs or the characteristics of three-dimensional instabilities. Our study aims to investigate the distinct instabilities that arise behind foils in side-by-side configurations due to the ground effect and wake interactions. The methodology for conducting this study is outlined in the Computational Methodology section, major observations are assessed in the

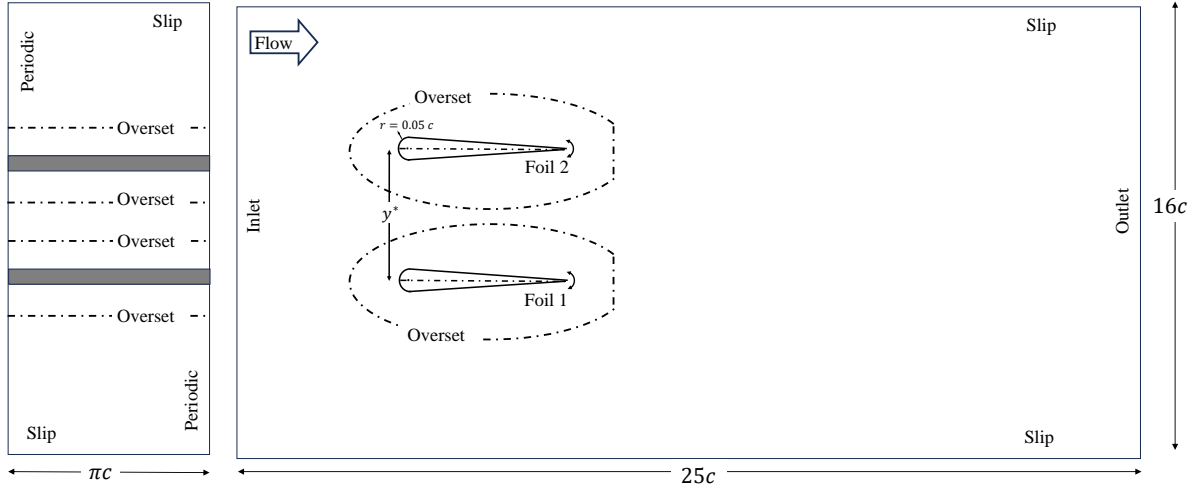


Figure 2. Dimensions of the computational domain with boundary conditions (not to scale). Here, y^* is the separation distance between the foils.

Results & Discussion section, and a brief summary of key findings is provided in the Conclusions & Summary section.

COMPUTATIONAL METHODOLOGY

The flow around two pitching foils in parallel (side-by-side) configurations were directly simulated at Reynolds number of $Re = 8000$. The separation distance between the infinite-span teardrop foils varied between $y^* = 0.5c$ and $y^* = 1.5c$ with increments of $0.25c$, where c is the foil chord (see figure 1). A sinusoidal pitching motion was prescribed on Foil 1 and Foil 2 as:

$$\theta_1(t) = \theta_0 \sin(2\pi ft), \quad (1)$$

$$\theta_2(t) = \theta_0 \sin(2\pi ft - \phi). \quad (2)$$

Here, θ_0 is the maximum pitching amplitude, f is the pitching frequency, t is time, and ϕ is the phase difference between foil motions. In-phase ($\phi = 0$) and out-of-phase ($\phi = \pi$) motions were considered in this study for Strouhal numbers of $St = fA/U_\infty = 0.3$ and 0.5 , where A is the tip-to-tip oscillation amplitude, and U_∞ is the freestream flow velocity.

Overset grid assembly implemented in OpenFOAM was used to simulate the oscillatory motion of the foils following Verma & Hemmati (2021). Rectangular computational domain extends $25c$, $16c$, πc in the streamwise (x -), cross-flow (y -), and spanwise (z -) directions, respectively. A non-homogeneous spatial grid with $\approx 4 \times 10^7$ hexahedral elements was utilized. Neumann boundary condition for both pressure and velocity was imposed at the outlet, uniform velocity boundary condition ($u = U_\infty, v = w = 0$) was imposed at the inlet, and slip boundary condition was imposed at the upper and lower boundaries of the domain. Surfaces of the foils were set to a no-slip wall boundary condition, and periodic boundary condition was utilized at the side walls.

RESULTS & DISCUSSION

We begin by investigating the cases of out-of-phase pitching foils operating under moderate ground effect ($y^* = 1c$)

for $St = 0.3$. Since the out-of-phase motion is mirror image symmetric, the bottom (Foil 1) and top (Foil 2) wakes exhibit symmetric features. Therefore, we only focus on the top foil for simplicity. Figure 3 illustrates the time evolution of vortical structures around the out-of-phase pitching foils at $St = 0.3$. The left column of figure 3 displays iso-surfaces of the Q-criterion on the upper surface of the top foil from a top-down perspective, while the right column of figure 3 shows the side view of contours of spanwise vorticity at the mid-plane ($z/c = 0$). An LEV is formed as a result of the upward stroke of the upper foil (see figure 3a-b). After its formation, it progresses downstream, while remaining attached to the surface. As a result of this interaction, a spanwise instability starts developing on the vortex at $t = 12.25P$ and becomes very prevalent at $t = 12.5P$. This phenomenon can be best explained with the method of images, which suggests that there is an opposite-sign image vortex forming beneath the surface that satisfies the no-slip boundary condition on the surface. Consequently, the LEV effectively forms a vortex pair with its opposite-sign image. Mutually induced velocities impose on them give rise to the amplification of the sinusoidal undulations on the vortex (Crow, 1970). The emergence of three-dimensional instabilities has been previously shown for vortex-wall interactions (Benton & Bons, 2014) as well as for single oscillating foils with combined heading and pitching motion (Chiereghin *et al.*, 2020; Verma *et al.*, 2023). However, this is the first study to identify them for purely pitching foils due to moderate ground effect. Moreover, the interaction of undulations with the surface lead to disintegration of the vortex before it reaches the trailing edge of the foil, as depicted in figure 3g-h. While the LEV on the lower surface of the top foil similarly exhibits spanwise undulations, its evolution is not detailed here for brevity, as it follows a comparable mechanism.

A noteworthy phenomenon occurs at the opposite end of the spectrum: instabilities vanish with severely intensified ground effect. The time evolution of vortex dynamics around the foils in extreme ground effect conditions ($y^* = 0.5c$) is depicted in figure 4 for $St = 0.3$. Similar to the moderate ground effect case, upstroke motion of the upper foil sheds an LEV. However, this LEV is markedly stronger, as demonstrated by a comparison between figure 3b and figure 4b. Additionally, a secondary structure with opposite sign vorticity forms beneath the LEV. It is worth noting that the moderate ground

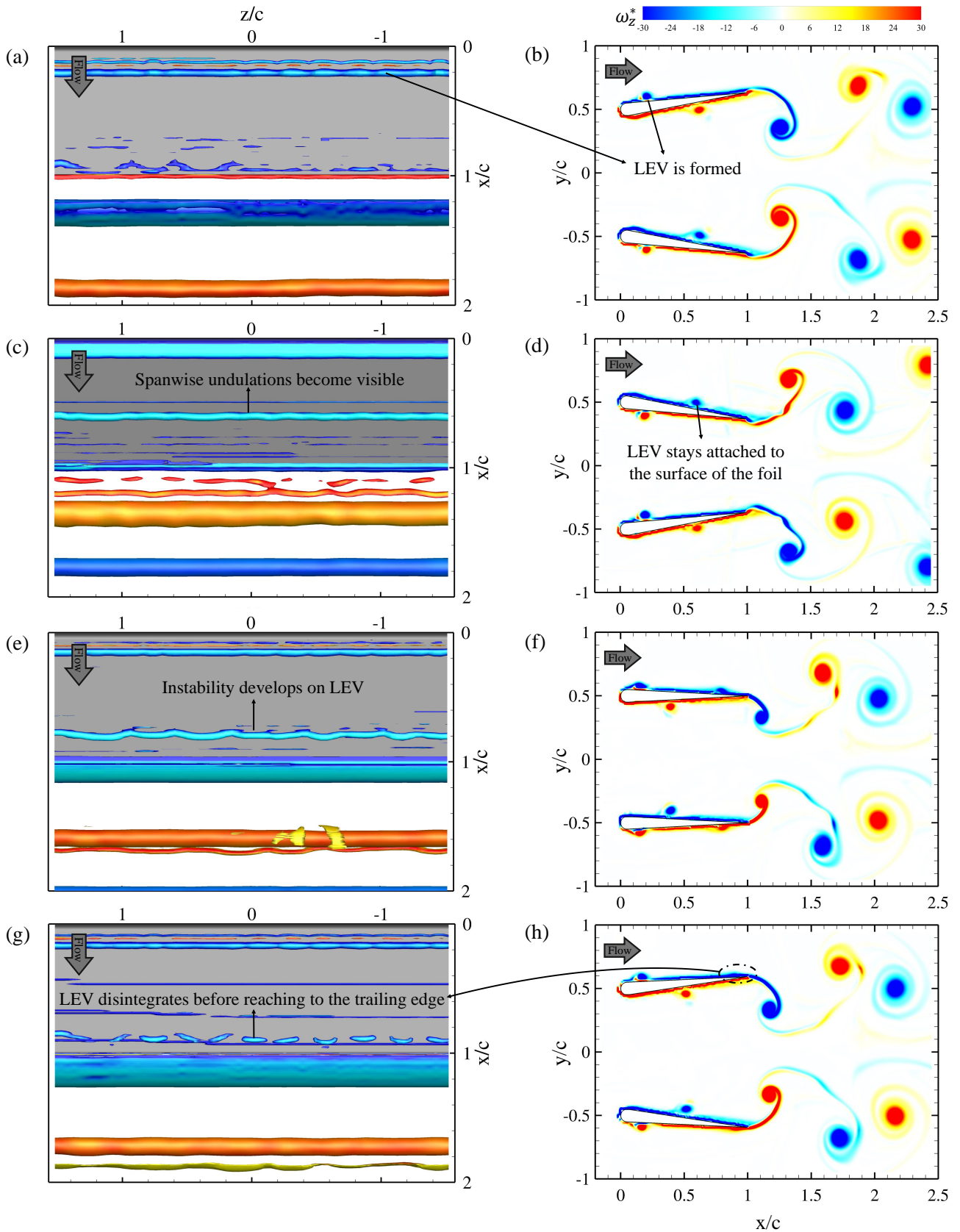


Figure 3. Temporal evolution of vortical structures around out-of-phase pitching foils for $St = 0.3$ and $y^* = 1c$ at (a,b) $t = 11.75P$, (c,d) $t = 12.25P$, (e,f) $t = 12.5P$, and (g,h) $t = 12.625P$. Here, ‘P’ is the period of the pitching cycle. Left column displays iso-surface of Q-criterion ($Qc/U_\infty = 5$) on the upper surface of the top foil viewed from above, while right column shows contours of spanwise vorticity ($\omega_z^* = \omega c/U_\infty$) at the mid-plane ($z/c = 0$).

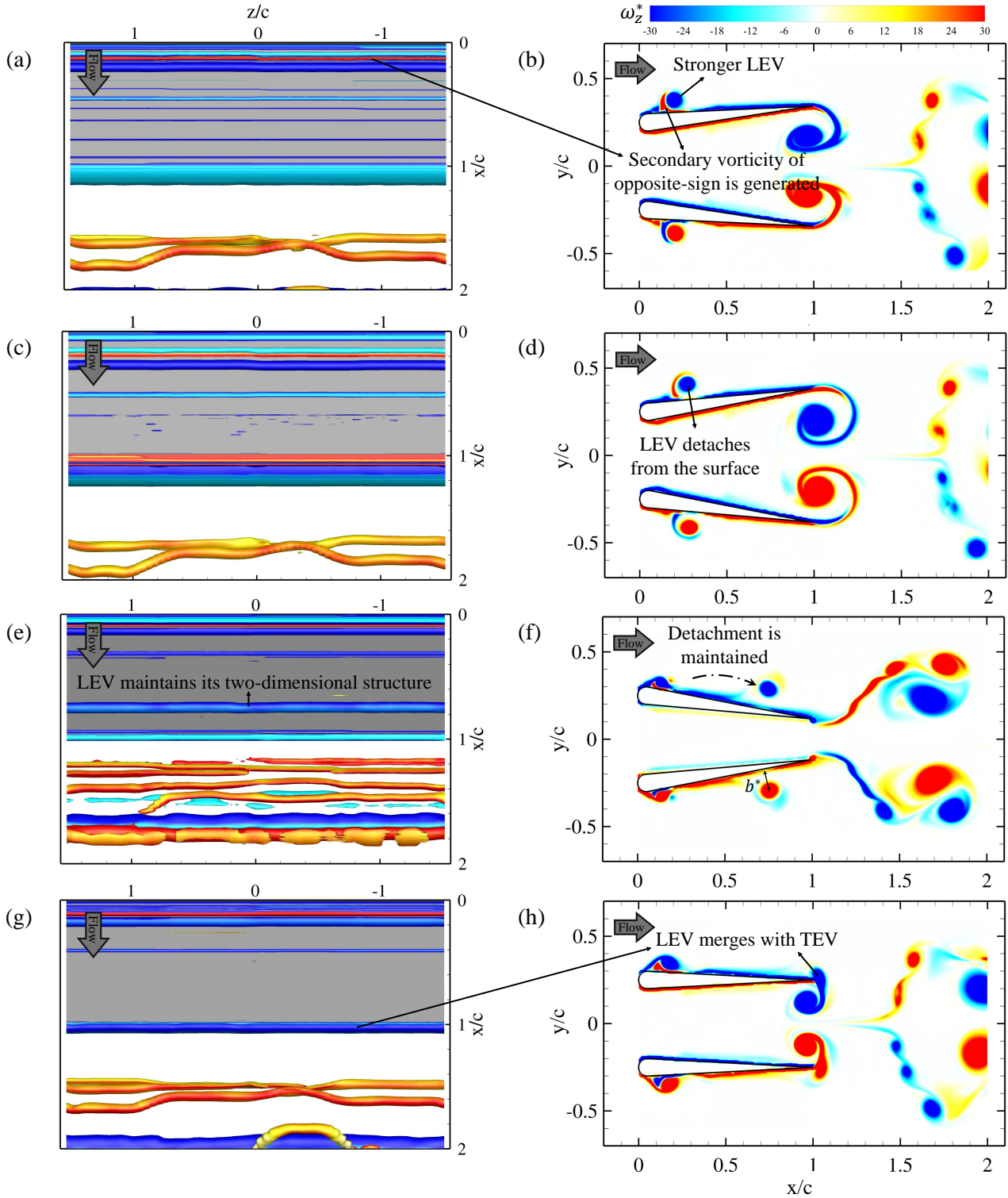


Figure 4. Temporal evolution of vortical structures around out-of-phase pitching foils for $St = 0.3$ and $y^* = 0.5c$ at (a,b) $t = 11.625P$, (c,d) $t = 11.75P$, (e,f) $t = 12.25P$, and (g,h) $t = 12.5P$. Here, ‘P’ is the period of the pitching cycle. Left column displays iso-surface of Q -criterion ($Qc/U_\infty = 5$) on the upper surface of the top foil viewed from above, while right column shows contours of spanwise vorticity ($\omega_z^* = \omega c/U_\infty$) at the mid-plane ($z/c = 0$).

effect case also presents secondary structure, but they are significantly weaker and barely visible in figure 3b. Interaction between a vortex and a wall leads to the detachment of the boundary layer from the surface, resulting in the formation of a secondary structure opposite to the main vortex (Quinn *et al.*, 2014; Leweke *et al.*, 2016). Vorticity budget analysis by Eslam Panah *et al.* (2015) shows that the flux of secondary

vorticity from the boundary correlates with the leading edge shear layer flux, which can explain the severity of differences between cases. The secondary structure induces an upward velocity, causing the detachment of the LEV from the surface (see figure 4). This resembles the interactive behavior of a vortex pair approaching a wall (Harvey & Perry, 1971; Peace & Riley, 1983), where the primary vortex rebounds from the

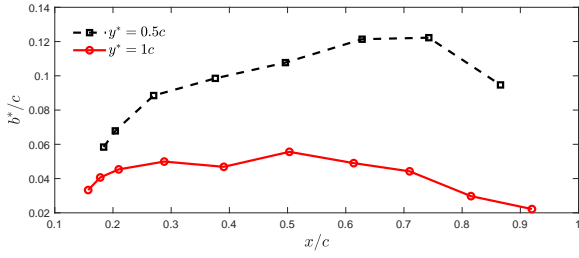


Figure 5. Separation distance (b^*) between LEV and foil surface at chordwise locations for the extreme ($y^* = 0.5c$) and moderate ($y^* = 0.5c$) ground effect cases at $St = 0.3$. The definition of b^* is illustrated in figure 4f.

wall due to a formation of the secondary vortex, a process often referred to as “vortex rebounding.” Subsequently, the LEV continues downstream, maintaining its distance from the surface until it merges with the newly developing TEV. Unlike the moderate ground effect case, the LEV does not exhibit any significant spanwise undulations and reaches the trailing edge as a two-dimensional vortex tube (see figure 4g). The dynamics of LEVs at higher Strouhal numbers exhibit similar characteristics, and thus are not explored in detail here. The main difference is that at $St = 0.5$, the foils generate stronger LEVs, resulting in detachment even at greater separation distances, covering the separation distance range considered in this study.

The comparison between extreme and moderate ground effect cases indicates that the detachment of the LEV from the foil surface is crucial in suppressing three-dimensional instabilities. This suppression is likely due to the diminished influence of the image vortex, which is formed due to the LEV’s proximity to the foil surface. This plays a central role in the emergence of three-dimensional instability. As the distance between the LEV and the foil increases, the effect of the image vortex weakens, effectively reducing the three-dimensional instabilities. This dynamic is consistent with theoretical models, which suggest that the growth rates of both long-wavelength and elliptic instabilities in a vortex pair are inversely proportional to the square of the separation distance between vortices (*b*) (Lewke *et al.*, 2016). Figure 5 illustrates the separation between the LEV and the foil surface (b^*), measured as the normal distance from the center of the LEV to the foil surface across chordwise positions for both scenarios. This highlights the influence of detachment on the emergence of three-dimensional instabilities. Another notable aspect of the LEV dynamics is the speed at which the detached vortex moves towards the trailing edge compared to its attached counterpart. The detached vortex reaches the trailing edge by $t = 12.5P$ (as shown in figure 4h), whereas the attached vortex remains at approximately $x/c \approx 0.8$ at the same time instant (as seen in figure 3f). Quinn *et al.* (2014) observed a similar lagging for a TEV in ground effect. This suggests that the slowing effect is attributed to the influence of the image vortex. The difference in streamwise velocities allows the attached vortex to stay under the influence of its image vortex for an extended period, thus promoting the development of spanwise undulations.

Both the emergence and suppression of three-dimensional instabilities are influenced by the ground effect. As the ground effect diminishes, i.e., as the separation distance between the foils increases, spanwise undulations on LEVs disappear (details not shown here for brevity). This underscores its role in the emergence of these instabilities. Conversely, the ground effect also plays a critical role in the suppression mechanism by significantly altering LEV dynamics (Gungor *et al.*, 2022).

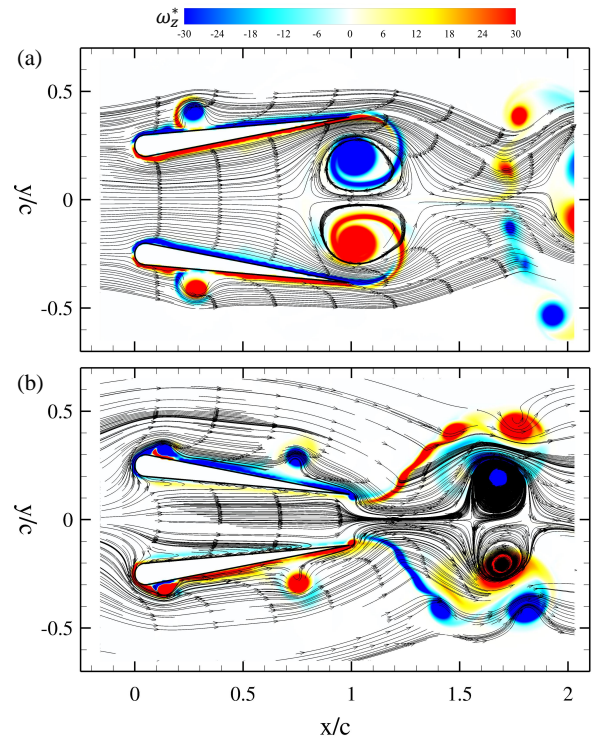


Figure 6. Streamlines around the out-of-phase pitching parallel foils for $y^* = 0.5c$ and $St = 0.3$ at (a) $t = 11.75P$, and (b) $t = 12.25P$. Here, ‘P’ is the period of the pitching cycle.

For out-of-phase motion, the strength of LEVs formed on the outer surfaces of the foils, i.e., the upper surface of the top foil and the lower surface of the bottom foil, is enhanced. However, the strength of LEVs on the inner surfaces, i.e., lower surface of the top foil and upper surface of the bottom foil, is diminished (Gungor & Hemmati, 2020). This dynamic is evident in figure 4, which shows that the top foil generates a stronger LEV on its upper surface, while shedding of the LEV from the lower surface is inhibited. This effect can be attributed to changes in the effective angle of attack due to induced velocity effects from the adjacent foil. Streamlines around the out-of-phase pitching parallel foils are presented in figure 6, illustrating that the effective angle of attack of the top foil at the beginning of the downstroke motion (figure 6a) is significantly larger compared to the angle at the beginning of the upstroke motion. This discrepancy leads to the formation of a stronger LEV on the upper surface, while inhibiting the formation of an LEV on the lower surface. This observation is consistent with findings of Wong & Rival (2015), who noted that the rate of growth of LEV circulation corresponds to the square of the effective flow velocity. Furthermore, Li *et al.* (2020) demonstrated that circulations of both the LEV and the secondary vortex increase with an increasing maximum effective angle of attack. This aligns perfectly with the current observations. Thus, extreme ground effect is associated with the suppression of LEV instabilities by enhancing the circulation of the secondary vortex beneath the LEV. This increased circulation leads to detachment of the LEV from the foil surface, resulting in the elimination of three-dimensional instabilities.

The suppression of LEV instabilities is also observed in in-phase pitching parallel foils operating under extreme ground effect conditions. However, this phenomenon is not explored in this study due to the unique differences between in-phase and out-of-phase motions. These differences signifi-

cantly impact the dynamics of LEVs, necessitating a dedicated investigation. Consequently, a comprehensive study focused on in-phase pitching motion will be the subject of our future research endeavors.

CONCLUSION & SUMMARY

The outcomes of this study reveal the presence of a distinct instability mechanism induced by ground effect on the LEVs of two pitching foils arranged side-by-side at $Re = 8000$. Under moderate ground effect, a spanwise instability develops on the LEVs that remain attached to the surface. This instability intensifies due to continuous and prolonged interaction between the LEV and the foil surface. This leads to disintegration of the LEV before it reaches the trailing edge. Contrarily, in the case of extreme ground effect, LEV detaches from the foil, reducing its interaction with the surface and thus preventing any spanwise instabilities. This detachment is facilitated by larger effective angle of attack, which amplifies the growth of secondary vortex beneath the shedding LEV. This effectively pushes the LEV away from the surface. These observations will be further substantiated through quantitative assessments to validate the critical role played by the ground effect in both fostering and suppressing these vortex instabilities.

REFERENCES

- Benton, S. I. & Bons, J. P. 2014 Three-dimensional instabilities in vortex/wall interactions: Linear stability and flow contro. In *52nd Aerospace Sciences Meeting*, p. 1267.
- Cerretelli, C. & Williamson, C. H. K. 2003 The physical mechanism for vortex merging. *J. Fluid Mech.* **475**, 41–77.
- Chiereghin, N., Bull, S., Cleaver, D. J. & Gursul, I. 2020 Three-dimensionality of leading-edge vortices on high aspect ratio plunging wings. *Physical Review Fluids* **5** (6), 064701.
- Crow, S. C. 1970 Stability theory for a pair of trailing vortices. *AIAA J.* **8** (12), 2172–2179.
- Deng, J. & Caulfield, C. P. 2015 Three-dimensional transition after wake deflection behind a flapping foil. *Physical Review E* **91**, 043017.
- Deng, J., Sun, L., Teng, L., Pan, D. & Shao, X. 2016 The correlation between wake transition and propulsive efficiency of a flapping foil: A numerical study. *Phys. Fluids* **28** (9), 094101.
- Eslam Panah, A., Akkala, J. M. & Buchholz, J. H. 2015 Vorticity transport and the leading-edge vortex of a plunging airfoil. *Exp. Fluids* **56**, 1–15.
- Gungor, A. & Hemmati, A. 2020 Wake symmetry impacts the performance of tandem hydrofoils during in-phase and out-of-phase oscillations differently. *Phys. Rev. E* **102**, 043104.
- Gungor, A., Khalid, M. S. U. & Hemmati, A. 2022 Classification of vortex patterns of oscillating foils in side-by-side configurations. *J. Fluid Mech.* **951** (A37).
- Harvey, J. K. & Perry, F. J. 1971 Flowfield produced by trailing vortices in the vicinity of the ground. *AIAA J.* **9** (8), 1659–1660.
- Leweke, T., Le Dizes, S. & Williamson, C. H. 2016 Dynamics and instabilities of vortex pairs. *Annual Review of Fluid Mechanics* **48**, 507–54.
- Leweke, T. & Williamson, C. H. 1998 Cooperative elliptic instability of a vortex pair. *J. Fluid Mech.* **360**, 85–119.
- Li, Z. Y., Feng, L. H., Kissing, J., Tropea, C. & Wang, J. J. 2020 Experimental investigation on the leading-edge vortex formation and detachment mechanism of a pitching and plunging plate. *J. Fluid Mech.* **901** (A17).
- Meunier, P., Le Dizes, S. & Leweke, T. 2005 Physics of vortex merging. *Comptes Rendus Physique* **6** (4-5), 431–450.
- Peace, A. J. & Riley, N. 1983 A viscous vortex pair in ground effect. *J. Fluid Mech.* **129**, 409–426.
- Quinn, D. B., Moored, K. W., Dewey, P. A. & Smits, A. J. 2014 Unsteady propulsion near a solid boundary. *J. Fluid Mech.* **742**, 152–170.
- Verma, S. & Hemmati, A. 2021 Evolution of wake structures behind oscillating hydrofoils with combined heaving and pitching motion. *Journal of Fluid Mech.* **927**, A–23.
- Verma, S., Khalid, M. S. U. & Hemmati, A. 2023 On the association of kinematics, spanwise instability and growth of secondary vortex structures in the wake of oscillating foils. *Proceedings of the Royal Society A* **479** (2276), 20230353.
- Wong, J. G. & Rival, D. E. 2015 Determining the relative stability of leading-edge vortices on nominally two-dimensional flapping profiles. *J. Fluid Mech.* **766**, 611–625.